Available online at www.sciencedirect.com
SCIENCE DIRECT
Diamond & Related Materials 15 (2006) 1276 – 1281
DIAMOND AND RELATED MATERIALS
www.elsevier.com/locate/diamond

Characteristics and surface energy of silicon-doped diamond-like carbon films fabricated by plasma immersion ion implantation and deposition

G.J. Wan [a,b], P. Yang [b], Ricky K.Y. Fu [a], Y.F. Mei [a], T. Qiu [a,c], S.C.H. Kwok [a], Joan P.Y. Ho [a], N. Huang [b], X.L. Wu [a,c], Paul K. Chu [a,*]

[a] Department of Physics and Materials Science, City University of Hong Kong, Tat Chee Avenue, Kowloon, Hong Kong, China
[b] College of Materials Science and Engineering, Southwest Jiaotong University, Chengdu 610031, China
[c] Department of Physics, Nanjing University, Nanjing 210093, China

Received 16 June 2005; received in revised form 28 July 2005; accepted 29 September 2005
Available online 21 November 2005

Abstract

Diamond-like carbon (DLC) films doped with different silicon contents up to 11.48 at.% were fabricated by plasma immersion ion implantation and deposition (PIII-D) using a silicon cathodic arc plasma source. The surface chemical compositions and bonding configurations were determined by X-ray photoelectron spectroscopy (XPS) and Raman spectroscopy. The results reveal that the sp^3 configuration including Si–C bonds increases with higher silicon content, and oxygen incorporates more readily into the silicon and carbon interlinks on the surface of the more heavily silicon-doped DLC films. Contact angle measurements and calculations show that the Si-DLC films with higher silicon contents tend to be more hydrophilic and possess higher surface energy. The surface states obtained by silicon alloying and oxygen incorporation indicate increased silicon oxycarbide bonding states and sp^3 bonding states on the surface, and it can be accounted for by the increased surface energy particularly the polar contribution.

PACS: 81.05.Uw; 68.35.Md; 52.77.Dq; M 81.70.−q; 68.03.Cd
Keywords: Si-doped DLC; Surface energy; Plasma immersion ion implantation and deposition; Contact angle

1. Introduction

Diamond-like carbon (DLC) films have favorable properties from the scientific and engineering points of view, but there are challenges in industrial applications due to the high residual compressive stress, poor adhesion to the substrate, poor thermal stability, and hydrophobic surface properties [1]. Alloying DLC films with Si has been reported to address some of the problems, for instance, improving the thermal stability, reducing internal stress, and enhancing wear and corrosion resistance as well as other mechanical properties [2,3]. However, the effects of silicon on the DLC properties largely depend on the fabrication conditions and have not been clearly established. For example, silicon-doped DLC (Si-DLC) films produced by plasma-enhanced chemical vapor deposition (PECVD) are likely saturated with hydrogen yielding some unsatisfying results in some applications as the Si–H bonds in the silicon containing precursor may not be broken down completely [2,4]. There have been few reports about Si-DLC films fabricated by elemental doping methods such as cathodic arc deposition, but in general, promising results have been obtained compared to those achieved by PECVD, particularly pertaining to the mechanical properties and thermal stability [3,5,6]. In this work, we employed plasma immersion ion implantation and deposition (PIII&D) in concert with a cathodic arc plasma source to produce Si-DLC films. The technique offers a number of advantages such as pure silicon plasma, high ionization efficiency, easy control of the implantation/deposition parameters by adjusting the bias voltages, and non-line-of-sight operation, making it an effective alternative for treating components possessing complex shapes [7]. Our literature search has not identified previous work on the fabrication of Si-DLC films employing this hybrid method. In many applications, the surface

* Corresponding author. Tel.: +852 27887724; fax: +852 27889549/+852 27887830.
E-mail address: paul.chu@cityu.edu.hk (P.K. Chu).

0925-9635/$ - see front matter © 2005 Elsevier B.V. All rights reserved.
doi:10.1016/j.diamond.2005.09.042

properties, particularly the surface free energy and surface tension, are very important. They affect important surface properties such as hydrophilicity, adhesion to the substrate, and adsorption behavior in many circumstances. In this paper, we report the characterization as well as surface energy investigation of the Si-DLC films produced by this hybrid technique.

2. Experimental details

Film deposition was conducted in our plasma immersion ion implantation and deposition (PIII&D) equipment that has been described in detail elsewhere [7–9]. P-type silicon (100) wafers were used as the substrate. The silicon plasma was generated by a cathodic arc plasma source composed of a pure silicon cathode. The triggering voltage was ~3 kV and the main arc current was maintained at around 120 A. The arc duration time was about 250 μs and the repetition frequency was 60 Hz. The emitted silicon plasma drifted through a 90° curved magnetic duct to eliminate deleterious macro-particles and was subsequently attracted to the silicon substrate biased at a −100 V DC (direct current). At the same time, acetylene gas was bled into the PIII&D chamber as the carbon precursor. The streaming silicon plasma collided with the C_2H_2 molecules causing partial ionization, and the films were deposited by reaction of ionized silicon with ionized acetylene and some unionized molecules. Different C_2H_2 gas flows were used to control the silicon doping content and the instrumental conditions are summarized in Table 1.

Raman spectra were acquired on a Renishaw RM3000 micro-Raman system with a laser source wavelength of 514 nm and the spectra were collected by scanning from 800 to 2200 cm^{-1}. X-ray photoelectron spectroscopy (XPS) was performed using a PHI 5600 equipped with a monochromatic Al K_α X-ray source (1486.6 eV) to determine the surface composition and chemical states.

The surface free energy was determined by a contact angle test using the sessile drop method on the JY-82 contact angle goniometer at ambient humidity and temperature. Doubly distilled water and five additional test liquids, glycerin, formamide, diiodomethane, glycol, and tritolyl phosphate, were used to determine the hydrophilicity as well as surface energy of the samples. In each test, six measurements were conducted on each sample taken from five different fields on the deposited wafer to obtain good statistics. The surface energy of the films was calculated using the Zimans and Good method [10] by combining the Young equation and the Van Oss equation of the work of adhesion [11,12]:

$$W_a = 2\left(\gamma_l^p \gamma_s^p\right)^{1/2} + 2\left(\gamma_l^d \gamma_s^d\right)^{1/2} = \gamma_l(1+\cos\theta), \quad (1)$$

where W_a is work of adhesion, θ is the contact angle, γ_l, γ_l^d and γ_l^p are the surface tension and its dispersive and polar components of the liquid phases, respectively, and γ_s^d and γ_s^p are the dispersive and polar components of the solid phases, respectively. Eq. (1) can be further simplified as:

$$\frac{\gamma_l(1+\cos\theta)}{2\left(\gamma_l^d\right)^{1/2}} = \left(\gamma_s^d\right)^{1/2} + \left(\gamma_s^p\right)^{1/2}\left(\frac{\gamma_l^p}{\gamma_l^d}\right)^{1/2} \quad (2)$$

By using the archival relative surface tension component values of the test liquids shown in Table 2 [10–12] and solving Eq. (2) with the contact angles measured from more than two test liquid/solid interfaces, we can obtain γ_s^d and γ_s^p. The surface tension is defined to be the sum of the dispersive γ_s^d and polar γ_s^p contributions. In our experiments, six test liquid/solid interfaces were chosen to obtain good statistics.

Table 1
PECVD instrumental parameters

Sample number	$F_{C_2H_2}$ (sccm)	Pressure (Torr)	Bias voltage (V)	Silicon arc source	
				Trigger voltage	Main arc current
# 1	20	4.0×10^{-4}	−100 (DC)	3 kV	120 A (250 μs, 60 Hz)
# 2	15	3.2×10^{-4}			
# 3	10	1.8×10^{-4}			
# 4	5	1.0×10^{-4}			

Table 2
Surface tension parameters of the test liquids at 20 °C

Liquid	γ_{LV}	γ_{LV}^p	γ_{LV}^d
Double distilled water	72.8	51.0	21.8
Glycol	48.3	19.0	29.3
Diiodomethane	50.8	2.3	48.5
Formamide	58.2	18.7	39.5
Tritolyl phosphate	40.9	1.7	39.2
Glycerin	63.4	26.4	37.0

3. Results and discussion

Raman spectroscopy is a common and powerful tool to study the structural properties of DLC due to the high scattering efficiency of the carbon-to-carbon bonding states. Fig. 1 shows the Raman spectra acquired between 800 and 2200 cm^{-1} from the Si-DLC films. All the spectra reveal a typical DLC structure characterized by one band composed of the main G (graphite) peaks and D (disordered) shoulder. This is in contrast to

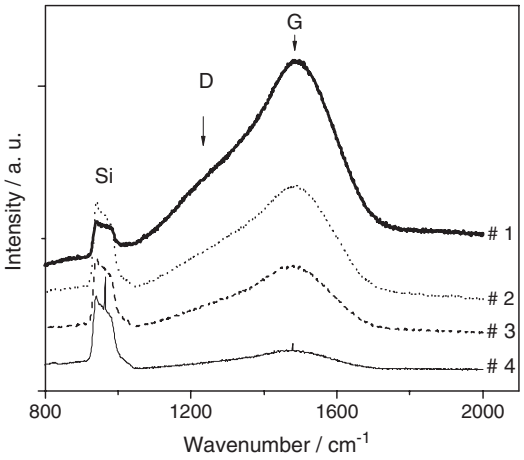

Fig. 1. Raman spectra of Si-DLC films produced by PIII&D.

graphite that typically shows two separate peaks at ~1550 and ~1350 cm^{-1} [13]. The Raman line shape changes to being less asymmetrical corresponding to the changes in the diamond-like structure with higher silicon content at decreased C_2H_2 partial pressure. All the main peaks show obvious low frequency shift compared to graphite, and a slight shift to a lower frequency for the G peaks can be observed. This is consistent with the increase in the diamond-like structure. On the other hand, the shift of the G band may be partially related to the de-straining action of silicon, and the shift of the D band arises from increased disorder due to increases in the averaged bond lengths [14]. Detailed deconvolution of the Raman spectra into the two peaks is useful to discern the DLC structure, for example, the sp^3 to sp^2 ratio, graphite cluster size, and extent of disorder [13]. Table 3 lists the fitted results of the Raman spectra of the Si-DLC films. The ratio of the Raman signal I_D/I_G is one important empirical factor to evaluate the carbon–carbon bonding states in the DLC film, and a smaller I_D/I_G value is commonly correlated with an increased sp^3 to sp^2 ratio [13,15]. We observe the decreased I_D/I_G trend with silicon doping increasing from samples # 1 to # 2 and # 4 and a small deviation in sample # 3 showing slightly higher I_D/I_G ratio than sample # 2. Nonetheless, it should be noted that the aforementioned relationship between the D and G bands in the Raman spectra is established for pure DLC films and not Si-DLC films, which should be more complicated. For instance, the Raman peak at approximately 1450 cm^{-1} associated with Si–C bonds can also affect the intensity and position of the G peak, albeit at a lower scattering efficiency [2], but on the other hand, the conspicuous second-order peak of the Si substrate at approximately 960 cm^{-1}, of which the intensity is proportional to the optical transparency of the film, produces errors in the deconvolution by affecting the background of the D peaks [3]. This may be the reason why some of the specific fitting parameters appear to be scattered. From this point of view, XPS may offer a more reliable analysis in this case because it provides more accurate information on the surface structures and bonding states of the films. In fact, it has been shown to disclose the structure of DLC and Si-DLC films more effectively [14,16,17].

The surface compositions of the Si-DLC films derived from the C1s, Si2p, and O1s photoelectron core level XPS spectra are listed in Table 4. Our results indicate that the Si dose is indeed increased by reducing the mass flow, that is, partial pressure of C_2H_2. It can also be observed that the oxygen content is negligibly low in the silicon doped film with the smallest silicon concentration, which is related to the small oxygen concentration in most DLC films, and that oxygen incorporation increases with higher silicon doping. The C1s spectrum is most useful in identifying the chemical states of the Si-DLC films. The surface chemical states of carbon in the Si-DLC films include mainly C═C (sp^2), C–C (sp^3), Si–C (sp^3), and C═O. As shown in Fig. 2, peak deconvolution is conducted by fixing the energies of the four bonding states at 283.3±0.1, 284.2±0.1, 285.1±0.1 and 286.5±0.1 eV, respectively [14–18]. The sp^3 fraction and two different sp^3 to sp^2 ratios calculated by sp^3 ([Si–C]+[C–C])/sp^2 ([C═C]) for the Si-DLC film, and sp^3 ([C–C])/sp^2 ([C═C]) for amorphous carbon reveal detailed bonding state changes in the films, as shown in Table 4. The results are plotted in Fig. 3 as a function of the C_2H_2 flow conditions. We can see that the sp^3 to sp^2 ratio of the former increases from samples # 1 to # 4 monotonically, and the latter increases from sample # 1 to # 2 first and then decreases slightly with silicon doping increasing. It can be concluded that silicon is likely incorporated in the film by replacing carbon atoms to form sp^3 bonds. At low silicon doping level, the sp^3 fraction for interlinks of DLC increases, as there are more induced disordered states of carbon–carbon bonds (including sp^3) by Si alloying. In contrast, at a high silicon doping concentration, Si incorporation can reduce the sp^3 fraction of interlinks of DLC by replacing carbon in the sp^3 matrix, while the overall sp^3 fraction including [Si–C] and [C–C] in the films increases, as shown in Table 4 and Fig. 3.

The configurations of silicon and carbon on the surface are likely more complicated due to the oxygen incorporating effects. To reveal more details, the Si2p and O1s XPS spectra were recorded. As shown in Fig. 4, the Si2p peaks of the Si-DLC films prepared under high C_2H_2 partial pressure with the smallest amount of silicon are relatively symmetric and centered around 100.5 eV due to Si–C bonding only [18,19]. The results indicate that no oxidation has occurred and very little oxygen is present on the surface. With increasing silicon concentration, the Si2p peaks of samples (# 2, # 3, # 4 increasingly) are more asymmetrical exhibiting a higher-shift shoulder that can be ascribed to silicon oxycarbide (SiO_xC_y:$SiOC_3$, SiO_2C_2 SiO_3C) bonding states [19,20]. It shows that some of the silicon atoms (or silicon carbide) on the surface combine readily with oxygen by the natural oxidation process. This can be further confirmed by the marked oxygen composition changes with higher silicon concentration. As shown in the O1s spectra in Fig. 4, oxygen forms both C═O (531.2±0.2 eV) and SiO_xC_y (532.3±0.2 eV) bonds and the latter becomes more noticeable at higher silicon concentration [20]. It should also be noted that oxidation will

Table 3
The fitting results of Raman spectra of Si-DLC films prepared by PIII&D

Sample no.	D-peak (cm^{-1})	G-peak (cm^{-1})	FWHM (D)	FWHM (G)	I_D/I_G
# 1	1289.5	1500.6	200.00	187.47	0.452
# 2	1275.2	1487.6	199.17	193.55	0.393
# 3	1291.7	1495.8	198.35	187.20	0.410
# 4	1258.2	1478.3	162.38	204.90	0.284

Table 4
Compositions of the Si-DLC films obtained by XPS, sp^3 to sp^2 ratio and sp^3 fraction calculated by deconvoluting of C1s spectra of the prepared films

Samples	Si (at.%)	O (at.%)	C (at.%)	sp^3 ([Si–C]+[C–C])/sp^2 ([C═C])	sp^3 ([C–C])/sp^2 ([C═C])	sp^3 fraction[a]
# 1	2.89	1.4	95.71	0.289	0.238	0.218
# 2	7.76	3.05	89.19	0.440	0.261	0.294
# 3	10.01	5.11	84.88	0.558	0.250	0.338
# 4	11.48	5.29	83.23	0.607	0.249	0.357

[a] sp^3 fraction represents $(sp^3[Si–C]+sp^3[C–C])/(sp^2[C═C]+sp^2[C═O]+sp^3[Si–C]+sp^3[C–C])$.

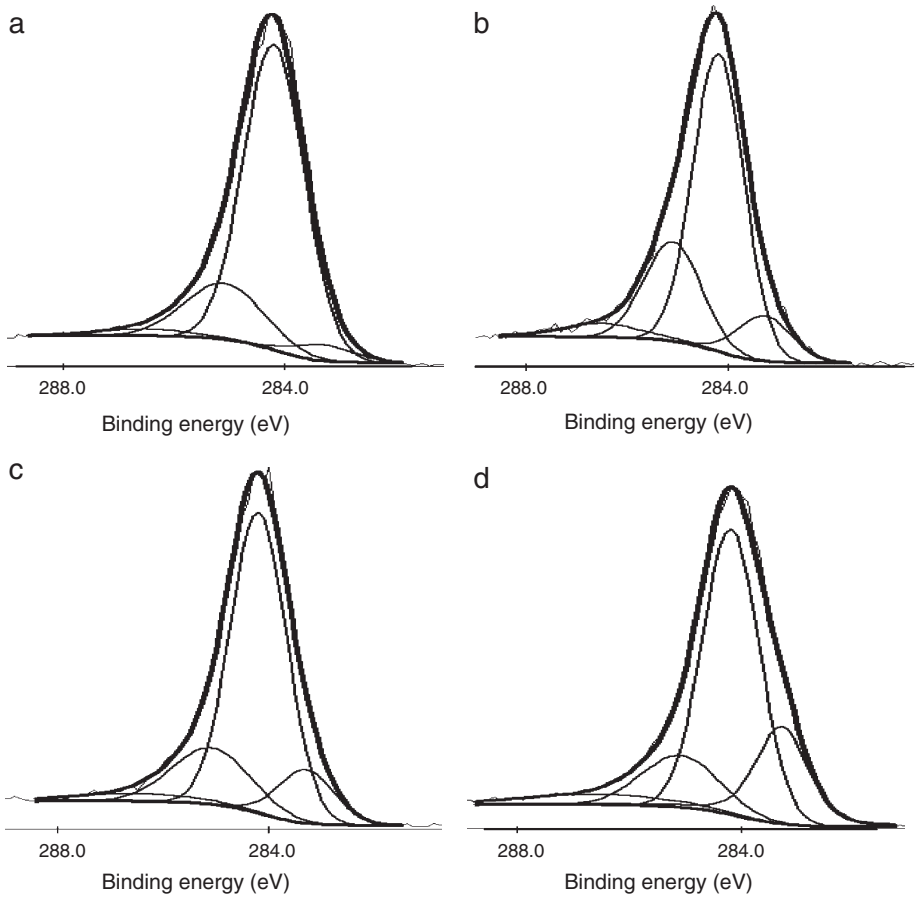

Fig. 2. Deconvoluted C1s core level photoelectron spectra of Si-DLC films produced by PIII&D: (a) sample # 1, (b) sample # 2, (c) sample # 3, and (d) sample # 4.

not affect the aforementioned conclusions on the sp^3 fraction, as silicon is known to form only the sp^3 bonding state even as silicon oxycarbide species.

The surface energy results reveal important thermodynamic properties of the films. In general, the higher the surface energy of the solid substrate relative to the surface tension of the liquids, the better is the hydrophilicity and the smaller is the contact angle as well as the better the adhesion to the substrate. Surface energy arises from the imbalance of the force between atoms or molecules at the interface. Several types of van der Waals interactions contribute to the surface energy that is dictated by two factors, dispersive γ^d and polar γ^p [10]. Fig. 5 shows the contact angles with water, surface energy, ratio of γ^p/γ^d and Si doping concentrations in the Si-DLC films as a function of the flow of C_2H_2 and deposition conditions. The water contact angles decrease and the surface tension increases monotonically with higher silicon concentrations indicating that our Si-DLC

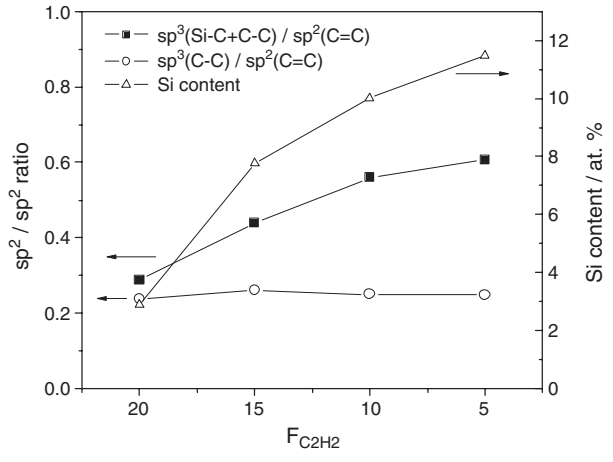

Fig. 3. sp^3/sp^2 ratio, silicon concentrations calculated by XPS of Si-DLC films and the relationship with C_2H_2 flow conditions.

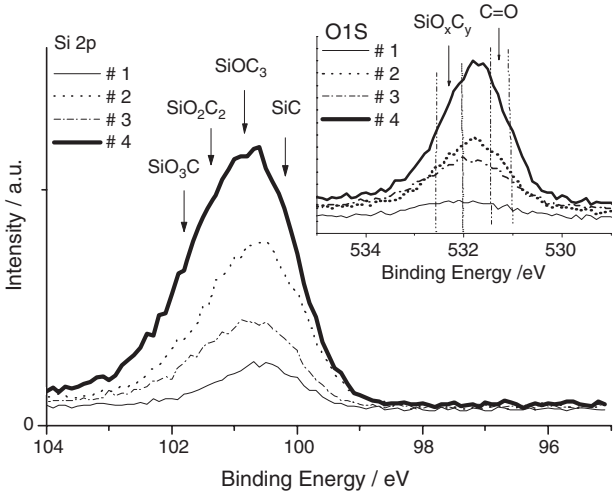

Fig. 4. XPS Si2p and O1s core level spectra of Si-DLC films prepared by PIII&D.

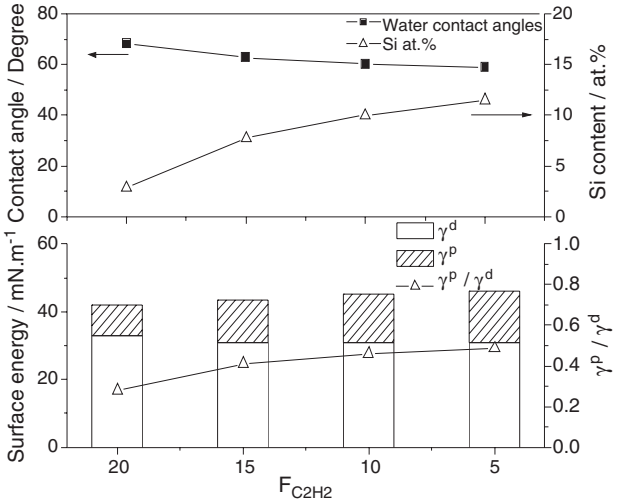

Fig. 5. Water contact angles, surface energy, γ^p/γ^d ratio and Si doping concentrations of the Si-DLC films and the relationship with flow rate of C_2H_2.

films with higher silicon concentration tend to be more hydrophilic. With regard to the surface energy, the two components vary and contribute differently. There is no obvious change in the dispersive components with higher silicon doping concentration, as the doses are relatively low without changing substantially the main interlinks of the carbon atoms as well as density of the films. The dispersive contribution is built up from a single interaction, which is generated by the movement of electrons around an atom or molecule depending largely on the kind and density of the materials. This effect should be insignificant in Si–C bonds compared to other bonding states because silicon and carbon are isoelectronic. The polar components increase obviously with higher silicon concentrations as shown in Fig. 5. Thus, the increased surface tension mainly arises from the higher polar contribution. The polar component is built up from different forces/interactions, like hydrogen bonds, covalent bonds and dipole–dipole interactions. The difference in the polar contribution to the total surface energy plays a critical role in determining the hydrophilicity for a polar liquid like water [10,21]. The increased polar contribution of the Si-DLC with increased Si contents is accordingly related to the surface bonding states obtained by silicon alloying and oxygen incorporation.

It should be noted that the Si-doped amorphous carbon materials reported in the literature appear to exhibit contradicting surface energy trends with increased silicon doping content, but it is well established that the surface properties depend critically on the preparation methods. To our knowledge [22,23], Si-DLC films produced by PECVD show decreased surface energy and are more hydrophobic with higher silicon concentrations. This is mainly ascribed to the substantially decreased dispersive component arising from excessive hydrogen bonding with silicon to form Si–H as well as increased defects such as vacancies that reduce the film density and change the electron distribution largely compared to silicon replacing carbon. Si-DLC films fabricated by a pure silicon doping method like cathodic arc or sputtering show consistent results and produce relatively high polar components compared to other DLC films or some metals (Ni, Ti, Al) doped DLC [24]. P. Zhang et al. conclude that the adsorption of oxygen on the surface plays an important role on the polar component of the metal doped DLC (a-C:Me) films including Si-DLC, and Si–O bonds contribute to the high polar component of a-C:Si films [24]. Similar results are observed in our case. The increased polar component of our prepared samples can be accounted for mainly by the surface states characterized by silicon oxycarbide bonding states. They are more polar than the silicon to carbon and carbon to carbon bonding states. The increased sp^3 configuration interlinks may contribute partly to it. More probably, some silicon atoms at the surface can readily form chemical bonds with oxygen without the hydrogen passivating effects as revealed in cases by PECVD.

4. Conclusion

Silicon-doped DLC films were produced by plasma immersion ion implantation and deposition (PIII&D) and cathodic arc plasma deposition. We observe increased sp^3 fraction configurations as well as more oxidation taking place on the Si-DLC films with higher silicon contents. The samples exhibit increased surface energy and become more hydrophilic with increased silicon doping content due to surface states obtained by silicon alloying as well as oxygen incorporation. This trend is dissimilar to that observed from films deposited using conventional PECVD. Our results address potentially the drawbacks of PECVD DLC in many applications. The increased surface energy of films prepared by this novel method should be beneficial to film adhesion particularly for DLC coatings in microelectronic and some biological applications. For instance, the more hydrophilic surface may enable the DLC film to produce a more effective anti-bacterial coating with 'conditioning' bio-films in vivo [25,26], and potentially better anti-thrombosis properties in blood contacting applications by reducing fibrinogen interactions with the film surface [22,27].

Acknowledgements

We would like to thank Dr. Wilson K. W. Wong of City University of Hong Kong for assistance in the XPS analysis. This work was financially supported by Hong Kong Research Grants Council (RGC) Competitive Earmarked Research Grant (CERG) #CityU 1120/04E, Hong Kong RGC and NSFC Joint Scheme N_CityU101/03, as well as NSFC No. 30370407 of China.

References

[1] J. Robertson, Prog. Solid State Chem. 21 (1991) 199.
[2] A.L. Baia Neto, R.A. Santos, F.L. Freire Jr., S.S. Camargo Jr., R. Carius, F. Finger, W. Beyer, Thin Solid Films 293 (1997) 206.
[3] C.S. Lee, K.R. Lee, K.Y. Eun, K.H. Yoon, J.H. Han, Diamond Relat. Mater. 11 (2002) 198.
[4] P. Papakonstantinou, J.F. Zhao, P. Lemoine, E.T. McAdams, J.A. McLaughlin, Diamond Relat. Mater. 11 (2002) 1074.

[5] J.R. Shi, X. Shi, Z. Sun, E. Liu, H.S. Yang, L.K. Cheah, X.Z. Jin, J. Phys., Condens. Matter 11 (1999) 5111.
[6] W.J. Wu, M.H. Hon, Surf. Coat. Technol. 111 (1999) 134.
[7] P.K. Chu, S. Qin, C. Chan, N.W. Cheung, L.A. Larson, Mater. Sci. Eng., R Rep. 17 (1996) 207.
[8] P.K. Chu, J. Vac. Sci. Technol., B 22 (1) (2004) 289.
[9] R.K.Y. Fu, Y.F. Mei, G.J. Wan, G.G. Siu, Paul K. Chu, Y.X. Huang, X.B. Tian, S.Q. Yang, J.Y. Chen, Surf. Sci. 573 (2004) 426.
[10] R.J. Good, J. Adhes. Sci. Technol. 2 (6) (1992) 1269.
[11] C.J. Van Oss, M.K. Chaudhury, R.J. Good, Chem. Rev. 88 (1988) 927.
[12] M. Amaral, M.A. Lopes, J.D. Santos, R.F. Silva, Biomaterials 23 (2002) 4123.
[13] A.C. Ferrari, J. Robertson, Phys. Rev., B 61 (20) (2000) 14095.
[14] J.F. Zhao, P. Lemoine, Z.H. Liu, J.P. Quinn, P. Maguire, J.A. Mc Laughlin, Diamond Relat. Mater. 10 (2001) 1070.
[15] B.K. Tay, X. Shi, H.S. Tan, H.S. Yang, Z. Sun, Surf. Coat. Technol. 105 (1998) 155.
[16] P. Mérel, M. Tabbal, M. Chaker, S. Moisa, J. Margot, Appl. Surf. Sci. 136 (1998) 105.
[17] J.X. Liao, W.M. Liu, T. Xu, Q.J. Xue, Carbon 42 (2004) 387.
[18] J.F. Moulder, W.F. Stickle, P.E. Sobol, K.D. Bomben, in: J. Chatain (Ed.), Handbook of X-ray Photoelectron Spectroscopy, Perkin-Elmer, Eden Prairie, MN, 1992.
[19] C.K. Park, S.M. Chang, H.S. Uhm, S.H. Seo, J.S. Park, Thin Solid Films 420–241 (2002) 235.
[20] R.P. Socha, K. Laajalehto, P. Nowak, Surf. Interface Anal. 34 (2002) 413.
[21] D.H. Kaelble, J. Moacanin, Polymer 18 (1977) 475.
[22] T.I.T. Okpalugo, A.A. Ogwu, P.D. Maguire, J.A.D. MuLaughlin, Biomaterials 25 (2004) 239.
[23] M. Grischke, A. Hieke, F. Morgenweck, H. Dimigen, Diamond Relat. Mater. 7 (1998) 454.
[24] P. Zhang, B.K. Tay, G.Q. Yu, S.P. Lau, Y.Q. Fu, Diamond Relat. Mater. 13 (2004) 459.
[25] A. Grill, Diamond Relat. Mater. 12 (2003) 166.
[26] A. Auditore, C. Satriano, U. Coscia, G. Ambrosone, V. Parisi, G. Marletta, Biomol. Eng. 19 (2002) 85.
[27] B. Ivarsson, I. Lundstrom, CRC Crit. Rev. Biocompat. 2 (1) (1986) 1.